

A COMPREHENSIVE APPROACH TO MODELING AND EVALUATING THE VISUAL ENVIRONMENT IN BUILDINGS

Vineeta Pal and Ardeshir Mahdavi
School of Architecture
Carnegie Mellon University
Pittsburgh, PA - 15213
U.S.A.

ABSTRACT

This paper describes the development, implementation, and evaluation of a computational tool for the comprehensive support of the lighting design process. The factors which are determined to be critical for this purpose, and which this study attempts to address, include a) consistent, coherent and first principles based underlying algorithms, b) the detailed modeling of the contextual parameters such as the sky and site conditions, c) provision of evaluation support for interpreting the computed data, d) the provision of active design support to explore the relationships between the design variables and the performance indices, and e) integration with other building performance simulation tools to encourage the exploration of inter-relationships between the energy aspects of lighting, thermal comfort, HVAC systems, and passive heating and cooling.

INTRODUCTION

This paper outlines an effort toward providing comprehensive computational lighting design support. This effort entails a unique synthesis of the following capabilities and features:

1. *First-principles based lighting modeling from schematic to final design phases:* A lighting simulation software is developed which uses a hybrid radiosity and ray tracing approach with extended form factors for the simulation of light propagation. Sky light is modeled by applying numeric integration methods to sky luminance distributions derived using advanced empirically based sky models.
2. *Detailed modeling of the context:* Five sky models (Perez, Kittler, Brunger, ASRC-CIE, Perraudeau) are implemented and comparatively analyzed using sky scanner data collected in Singapore.
3. *Design evaluation support:* Design evaluation support is provided by aggregate performance indicators such as glare and uniformity indices, besides illuminance and luminance for all surfaces.

4. *Active lighting design support:* A preference-based approach in conjunction with an investigative projection technique is used for performance-driven design exploration. Individual or multiple performance variables (glare, uniformity, minimum illuminance, average illuminance, etc.) can be used for deriving the design evolution trajectory.
5. *Integration with other simulation tools:* The lighting simulation module is integrated within a larger software environment (SEMPER) for the prediction and evaluation of multiple performance indicators (for energy, light, acoustics, etc.) in buildings. The building representation needed for lighting simulation and analysis is directly derived from the design representation (shared object model) in the SEMPER environment using a homology-based mapping technique.

We also present an evaluation of the tool using measured data in a test space with complex geometry and a dynamic facade with movable devices.

THE COMPUTATIONAL ENGINE

The computational engine uses a first-principles based light modeling algorithm which is not only applicable to geometrically simple environments with diffusely reflecting surfaces but also to non-orthogonal geometries with obstructions and surfaces with complex reflectance and transmittance functions. The objective is to use the same detailed modeling approach at any stage of the design process without falling back on simplified procedures in the early stages of design due to the low design resolution. This is also applied to the modeling of the contextual parameters, such as the climatic and site conditions, via the use of detailed sky models along with a system for a detailed description of the site surroundings.

MODELING LIGHT TRANSFER

A radiosity based approach, using extended form factors to take into account specular reflections (Tellier and Bouatouch 1991) is used for modeling light transfer. This model was extended to take into account transmitting surfaces. The environment is numerically

discretized into small patches and a system of radiative balance equations (Eq. 1) is derived for all patches and solved. In the computation of the form factors, the algorithm enters into a recursive ray-tracing mode whenever a specular surface is encountered. Thus, intermediate patches can contribute to the form factor between two patches by specularly reflecting light from one to the other.

$$L_i^d = L_i^E + \sum_j \text{EFF}_{ji} \cdot L_j^d \quad \text{Eq. 1}$$

where L_i^d global diffuse radiance of patch i
 L_i^E self emitted radiance of patch i
 EFF_{ji} extended form factor from j to i
 L_j^d global diffuse radiance of patch j

In Figure 1, the surface patches j and k contribute to the extended form factor between patch i and patch m by specularly reflecting light from i onto m .

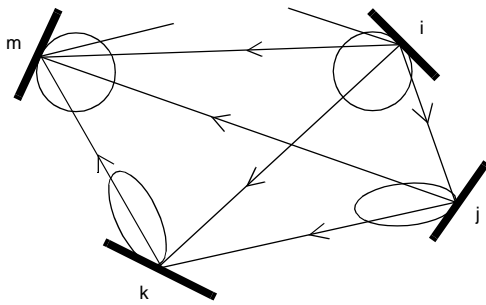


Figure 1. Graphical representation of the computation of extended form factors.

Progressive radiosity is used to solve the system of radiative balance equations which are thus derived.

MODELING SKY LIGHT

The sky dome is discretized into a matrix of patches, the center of each patch being geometrically located in terms of its altitude (θ) and azimuth (ϕ). Any one of five sky luminance modeling algorithms (Perez, Kittler, Brunger, ASRC-CIE, CIE) can be used to derive the relative sky luminance for the center of each of these sky patches. If the outdoor horizontal diffuse illuminance is known, either from measurement or from weather files, the relative sky luminance for each patch can be normalized using the horizontal diffuse illuminance to obtain the absolute sky luminance distribution pattern.

The sky patch visible through a discretized window patch is determined for a particular reference point and its contribution (as per its absolute luminance) is integrated into the total sky component for that reference point. The integration is performed over all

sky patches visible from the reference point. Thus, given a sky luminance distribution, the interior illuminance due to the sky contribution E_i at a reference point on a horizontal surface is given by:

$$E_i = \int_{\phi_1, \theta_1}^{\phi_2, \theta_2} \cos\theta \sin\theta \cdot L_{\theta, \phi} \cdot \tau_{\omega} d\theta d\phi \quad \text{Eq. 2}$$

where $L_{\theta, \phi}$ absolute luminance of the sky point
with altitude of θ and azimuth of ϕ
 τ_{ω} glazing transmittance

External obstructions are treated by projection of their outlines onto the virtual sphere. The luminances of the occluded sphere patches are replaced by those of the obstructions. For this purpose, the radiosity solution for the external surfaces has to be obtained before the radiosity solution for the internal surfaces can be calculated. The alternative is to solve a very large system of radiative balance equations for all interior as well as exterior surface patches. In a complex environment the number of patches can grow unmanageably. In response to this problem we make the assumption that the interior surfaces have an insignificant contribution towards the illumination of the exterior surfaces. This allows us to break up one large system of equations into two smaller systems of equations - one for exterior surfaces and one for interior surfaces. After the radiosity solution for the external surfaces has been obtained, their contribution to the illumination of the interior surfaces can be computed.

EVALUATION OF SKY MODELS

For a reliable prediction of illuminance and luminance distribution in daylight interiors, detailed data on the availability of daylight in general and the luminance distribution of the sky in particular are necessary. We performed a comparative assessment of five sky luminance models in view of their applicability in the tropical context, using measured data in Singapore (Mahdavi et al. 1998a). The five sky luminance distribution models considered were:

1. CIE standard overcast sky (CIE 1973).
2. All weather sky model (Perez et al. 1993).
3. ASRC-CIE model (Perez et al. 1990).
4. Brunger's model (Brunger 1987).
5. Kittler's model (Kittler 1986).

The results are given in Figure 2 which shows the mean relative errors with a deviation range which contains 70% of all relative error values.

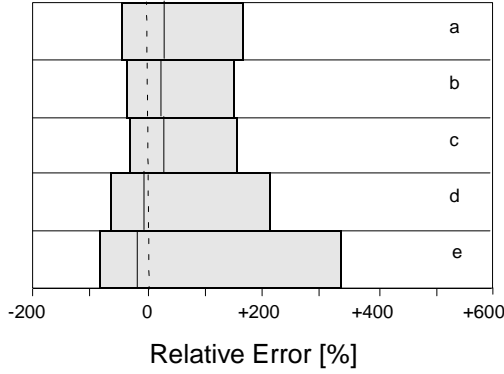


Figure 2: Mean Relative Errors with the corresponding Deviation Ranges containing 70% of the relative errors. (a: CIE, b: Perez, c: Kittler, d: Brunger, e: ASRC-CIE)

DISCUSSION:

Based on the available empirical data of the sky conditions in Singapore, the following provisional conclusions were derived by the study:

1. Based on the criteria of "high correlation" and a "small error range", the Perez and Kittler models perform better in the prediction of Singapore's sky luminance distribution.
2. The majority of the models display a tendency toward overestimating the sky luminance values, particularly in the sky region further away from the sun position.
3. There is not much variation in the models' predictive performance over the various sky conditions, with the exception of the CIE standard overcast sky model which has a predictably poor performance under clear sky conditions.

DESIGN EVALUATION SUPPORT

For the purposes of design evaluation, it is helpful to summarize the large amounts of illuminance and luminance data generated by the simulation tool into aggregate performance indicators such as glare and uniformity indices. It is also necessary from the perspective of conforming to codes and design guidelines which are sensitive to the issue of visual comfort and daylighting in buildings and which prescribe ranges for these indicators. In response to this requirement various glare indices (DGI, Hopkins 1971; CGI, Einhorn 1979; and UGR, Sorenson 1991) and uniformity indices are implemented as a part of the lighting model.

Three examples of uniformity indicators are implemented. The first is taken from Hentschel 1982 and is given by:

$$\text{uniformity} = \frac{E_{\min}}{E_m} \quad \text{Eq. 3}$$

where E_{\min} is the minimum (horizontal) illuminance and E_m is the average (horizontal) illuminance.

This indicator involves, per definition, numeric values of light levels at a single point. Occasionally it has been argued that the reliability of the so derived uniformity indicator can be affected due to the uncertainties involved in obtaining the individual illuminance level at a certain point.

In response to this, a number of statistically more elaborate indicators have been proposed as second generation uniformity indicators. One of these proposals (Mahdavi et al. 1995) has been implemented. It provides the following definition for the illuminance distribution uniformity factor and delivers uniformity attributes between 0 and 1:

$$U = \frac{E_m}{E_m + E_{SD}} \quad \text{Eq. 4}$$

where E_{SD} is the standard deviation and E_m the average value of the illuminance levels.

However, as with all second generation indicators, the uniformity indicator of Eq. 4 has a limitation. It is indifferent to the specific topological pattern of adjacent illuminance (or luminance) patterns. Therefore, certain fields which have obviously different distribution patterns yield identical uniformity attributes no matter if first or second generation indicators are applied (Mahdavi and Pal 1998b).

In response to this problem, a third uniformity indicator was proposed by Mahdavi and Pal 1998b as the concept of a single-number "entropic distribution index" (EDI). For a rough approximation of the entropic distribution index (EDI) of a two-dimensional orthogonal field with n grid elements (with corresponding illuminance levels E_i), the following formulation was proposed:

$$\text{EDI} = \frac{100}{n} \sum_{i=1}^n (P_{i,g} \cdot P_{i,l})^{0.5} \quad \text{Eq. 5}$$

where $P_{i,g}$ and $P_{i,l}$ are the global and local probability terms as per the following definitions:

$$P_{i,g} = 1 - \frac{|E_i - E_{m,g}|}{E_{m,g} + E_{sd}} \quad \text{Eq. 5}$$

$$P_{i,l} = 1 - \frac{|E_{m,l,i} - E_{m,g}|}{E_{m,g} + E_{sd}} \quad \text{Eq. 7}$$

where E_i is the illuminance level at point i , $E_{m,g}$ is the average illuminance of the whole field, E_{sd} is the standard deviation of the illuminance levels of the whole field, and $E_{m,l,i}$ is the local average of the illuminance levels in the immediate neighbourhood of the point i .

The EDI was implemented and the evaluative potential of the various uniformity indices was explored. We showed a clear potential for an entropy-based measure of light distribution uniformity as it can address the extreme value dependency of the first generation uniformity indicator (Eq. 3) and the topological indifference of the second generation uniformity indicator (Eq. 4) (Mahdavi and Pal 1998).

EMPIRICAL EVALUATION

One of the evaluation studies was performed in the Intelligent Workplace (IW). This is a recently established laboratory at the Carnegie Mellon University campus for demonstration and hands-on study of advanced building systems/technologies and their integration. The western section of a south bay in IW is dedicated to daylight studies (Figure 3). This area is partitioned from the rest of IW using white-colored partitions. About 60% of the external wall of the space consists of glazing. The facade system includes a set of three parallel external moveable louvers which can be used for shading purposes and - to a certain degree - for light redirection and transmission purposes. Continuous illuminance measurements have been performed between December 1997 and December 1998. Outdoor light conditions are monitored using a total of 11 illuminance and irradiance sensors that are installed on the daylight monitoring station on the roof of the IW.

To empirically evaluate the lighting model's performance, the illuminance levels at the 10 sensor positions in the test space were both measured and simulated for various times/dates and louver positions. Measured global and diffuse outdoor irradiance values were used to derive the sky luminance distribution. Quality control of the measured data was carried out before selecting the time periods for which the simulations were done. A total of 1080 data points (108 hours, 10 sensors) were used for the evaluation. Figure 4 shows the mean relative errors of the simulation for this data set.

Figure 5 shows the distribution of errors. In general, the lighting model's predictions of indoor light levels match the measurements quite well. Detailed inspection of the results showed that predictions under clear sky conditions are not as accurate as those for cloudy conditions. The reasons for this and approaches to further enhancement of the simulation tool are currently being explored.

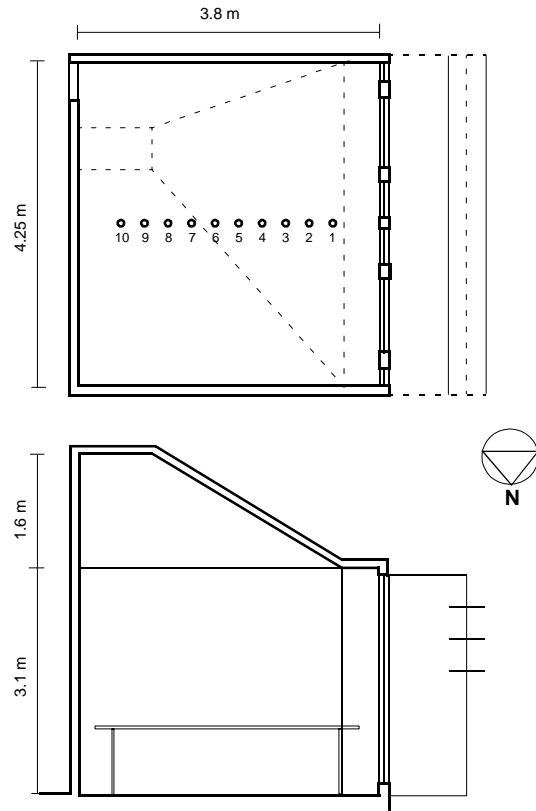


Figure 3: Plan and section view of the test space.

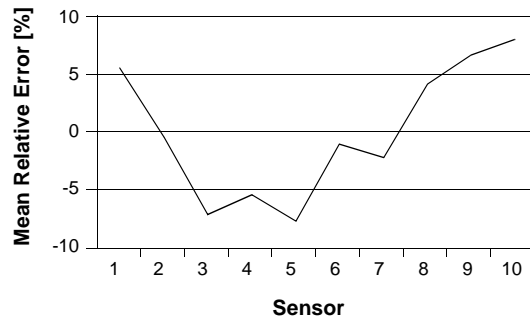


Figure 4: Mean relative errors for the 10 sensor positions.

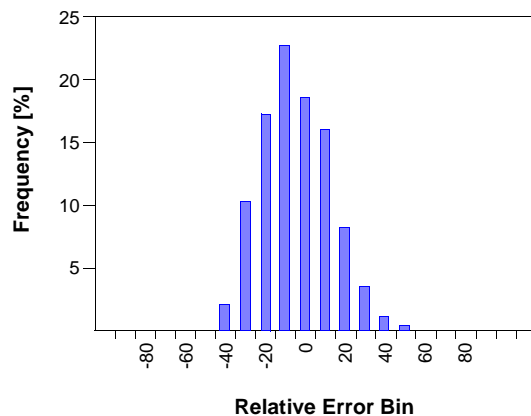


Figure 5: Histogram showing the distribution of relative errors.

ACTIVE DESIGN SUPPORT

Conventional simulation tools are "mono-directional" in the sense that a particular set of design attributes (formal, semantic, and contextual) is translated into a "unique" set of results or performance indicators. They do not support moving in the other direction, i.e., in the generation of possible configurations of design attributes to achieve required performance indices.

In order to address this requirement, Mahdavi and Berberidou 1994, developed the concept of a bi-directional inference mechanism which could enable the designer to generate partial design configurations based on desired performance indices. To deal with the issue of ambiguity inherent in the one-to-many mapping between the performance indicator and the design configurations, a preference based convergence strategy is applied. Thus a preference scale can be defined for any design variable which can be assigned successive degrees of preference ratings for a well defined set of continuous or discrete values it can assume. The preference structure and constraints may be specified by the user or can be derived based on empirical studies, codes, standards and other technical literature.

In a preference-based convergence approach for bi-directional analysis, a preference index D_p , for a design variable D_v can be defined if and only if D_p can be expressed as a function of D_v :

$$D_p = f(D_v) \quad \text{Eq. 8}$$

After the preferences are defined, the bi-directional inference engine uses an iterative approach or "investigative projection technique" (Mahdavi and Berberidou 1994) which iteratively moves towards a preferable design using a quasi-greedy procedure. The objective is to achieve the desired performance change by increasing the preference attributes of the variables with the lowest current preference attributes, or - in case these preferences cannot be increased - to achieve the desired performance change by decreasing the preference attributes of the variables with the highest current preference attributes. An example is given below as an illustration of the use of active design support.

Three cases are presented here where the user explores the tradeoffs between the design variables of overhang depth and glazing area in terms of average illuminance, uniformity and glare within a room. The preference values for the two design and three performance variables are shown in Table 1. The values used for the preferences are for illustrative purposes only. The user may choose to use a different set of preferences if desired. The base-case design is shown in Figure 6.

Table 1: Preferences for performance and design variables.

	Preference [-]				
	0	0.6	1	0.6	0
Glz. Area [m ²]	1	4	5	6	7
Ov. Depth [m]	0.1	0.5	1	1.2	1.5
Avg. illum [lx]	0	200	1500	3000	10000
Uniformity [-]	0	0.5	1	-	-
Glare [-]	-	-	0	15	30

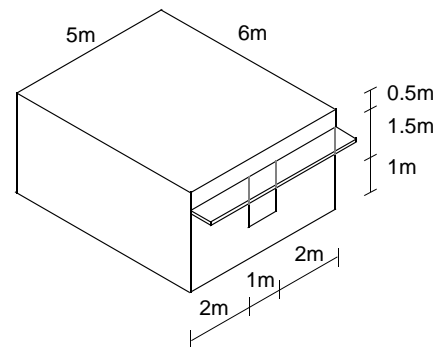


Figure 6: The base-case design configuration. (Overhang depth is 0.3 m)

In the first case, the design exploration is driven by the objective of maximizing the average preference for uniformity (Eq. 4), average illuminance, and daylight glare (DGI). Equal weights are given to the three performance variables in taking their average preference. The design evolution trajectory given in Figure 7 shows that the average preference of the performance variables can be improved by increasing the glazing area and reducing the overhang depth from the base case.

In the second case, the design evolution is guided by the objective of improving the average illuminance alone. The results are shown in Figure 8. The average illuminance is increased by increasing the glazing area and reducing the overhang depth. However, the average illuminance is brought closer to the desired 1500 lx by then increasing the overhang depth.

In the third case, the design evolution is driven by the objective of improving the uniformity. The results are shown in Figure 9. Both the glazing area and the overhang depth increase to achieve this objective.

The base-case and the final designs according to the three different objectives are shown in Figure 10.

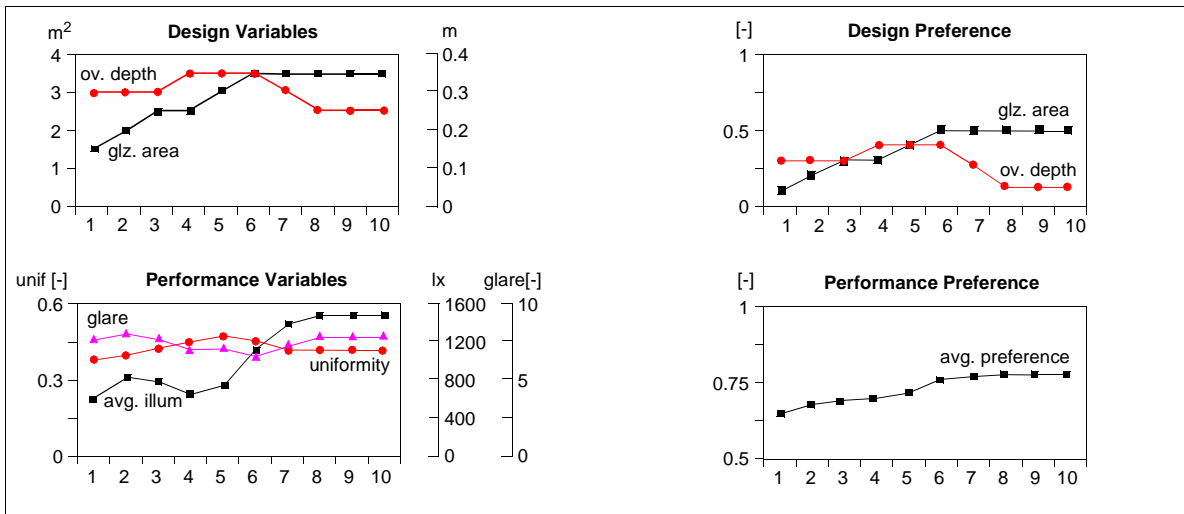


Figure 7: The design and performance trajectory for 10 iterations for Case 1.

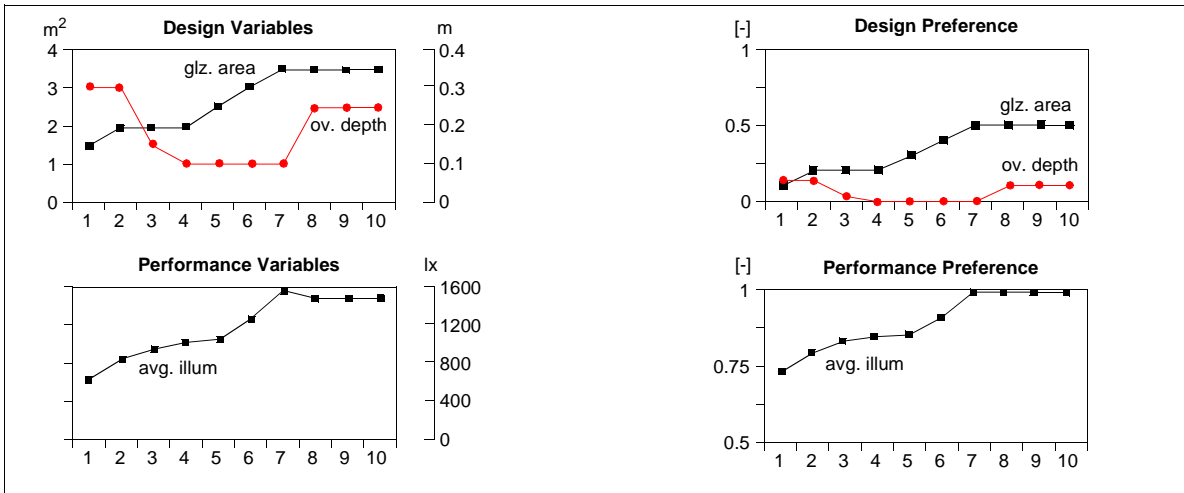


Figure 8: The design and performance trajectory for 10 iterations for Case 2.

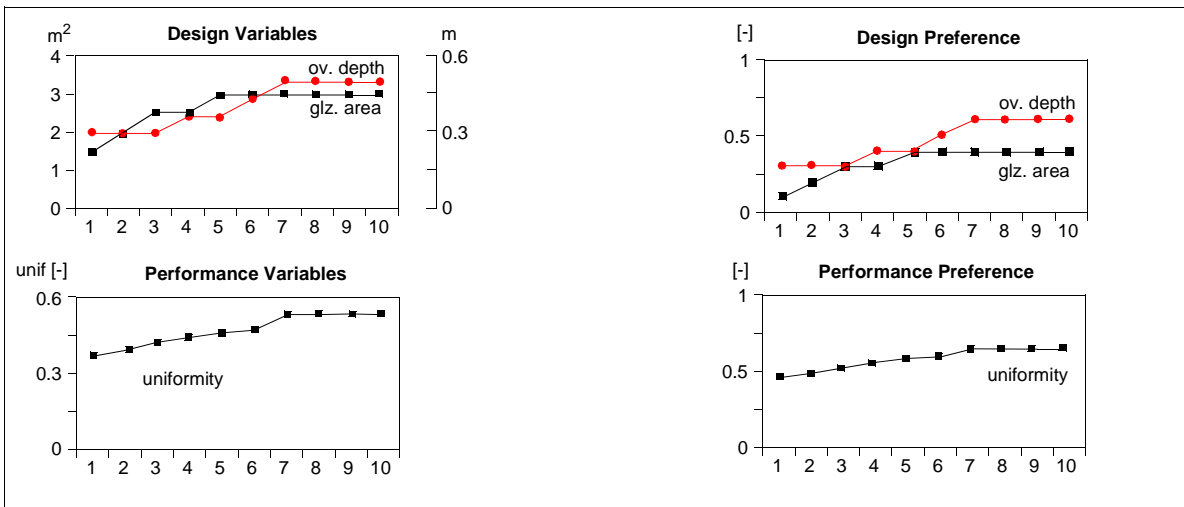


Figure 9: The design and performance trajectory for 10 iterations for Case 3.

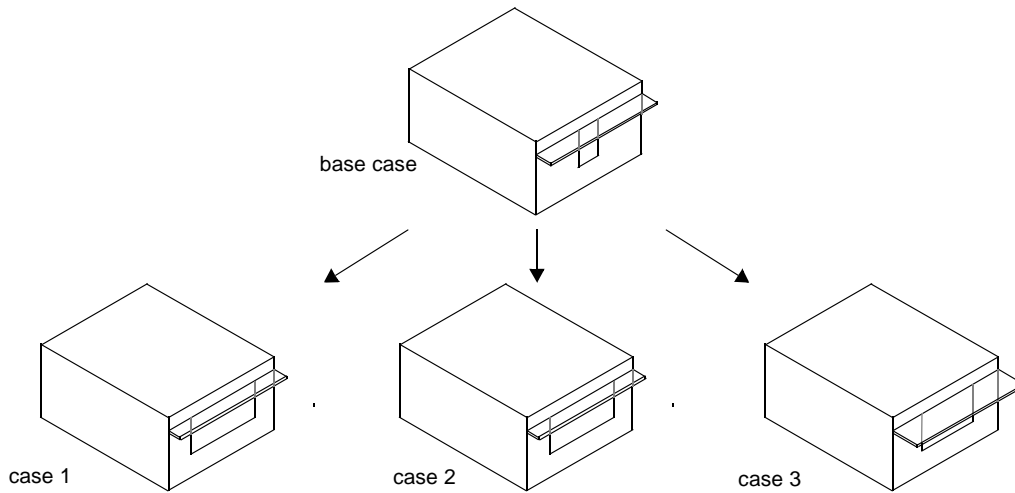


Figure 10: The base-case and the recommended design based on the three different criteria of the cases explored.

INTEGRATION WITH OTHER TOOLS

The lighting simulation tool is integrated within a larger software environment (SEMPER) which is being developed for the prediction and evaluation of multiple performance indicators (for energy, light, acoustics, etc.) in buildings (Mahdavi 1996). SEMPER incorporates an object-oriented, space-based shared building representation, with dynamic links to different building performance evaluation applications. It is thereby intended to computationally support the evaluation of buildings across multiple performance mandates concurrently, with a view toward achieving total building performance and systems integration.

The overall architecture of SEMPER is shown in Figure 11. All applications in SEMPER share a common object model (SOM) which reflects the building representational requirements of seven simulation modules and is implemented in Java. Each application may have a number of application-specific objects within its own object model. The dynamic links between applications occur at the object model level through mechanisms such as derived values, thereby, avoiding direct links between application data structures. This use of a shared object model, but with independent data structures for each application, allows the individual applications to be developed fairly independently, while still communicating in an effective manner.

The building representation needed for lighting simulation and analysis is directly derived from the design representation (shared object model) in the SEMPER environment using a homology-based mapping technique. Figure 12 shows the mapping between the

shared object model in SEMPER and the lighting domain object model.

The shared object model has knowledge of architectural spaces as well as their constituents (enclosure elements) and their relationships (adjacencies, shared walls/roofs, etc.). The lighting domain receives this information and can associate surface layers with each enclosure, opening, attachment, or partition element. The surface layers include information on surface reflectance and transmission properties. These surfaces can then be segmented into smaller grid elements to facilitate the radiosity solution. No user intervention is required to map subsequent changes in the architectural representation to the lighting model. Similarly, the lighting results can be used by other domains (e.g. the electrical lighting power consumption can be used by the energy module) without user intervention.

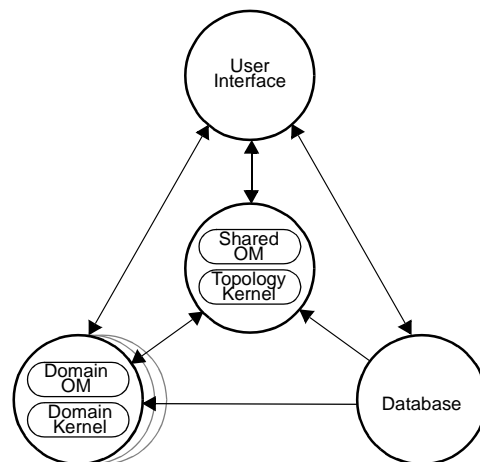


Figure 11: Schematic Representation of the Architecture of SEMPER

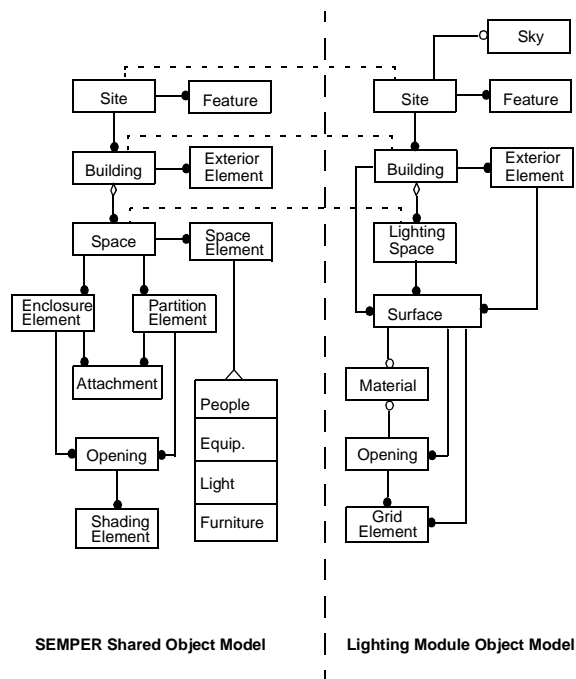


Figure 12: Mapping between the shared object model and lighting domain object model.

CONCLUSIONS

This paper has given an overview of the development of a lighting simulation model within a software environment which *a)* uses consistent, coherent and physically-based algorithms, *b)* provides active design support and design evaluation support, and *c)* supports the process of integrated design of building systems. Future work includes adding a user interface for the lighting module and further validation studies.

ACKNOWLEDGMENTS

The authors acknowledge the support of the Advanced Building Systems Integration Consortium (ABSIC), Center for Building Performance and Diagnostics (CPBD), School of Architecture, Carnegie Mellon University, toward completion of the research presented in this paper.

REFERENCES

Brunger, A. P. (1987). "The Magnitude, Variability and Angular Characteristics of the Shortwave Sky Radiation at Toronto". University of Toronto, Ph.D. Thesis.

Commission Internationale de l'Eclairage (1973). "Standardisation of Luminous Distribution of Clear Skies". CIE Publication No. 22, Paris: CIE.

Einhorn, H. D. (1979). "Discomfort Glare: A Formula to Bridge Differences." *Lighting Research and Technology*, Vol. 11, No. 2, p. 90.

Hentschel, H. (1982): *Licht und Beleuchtung; Theorie und Praxis der Lichttechnik*. Dr. Alfred Hüthig Verlag Heidelberg.

Hopkinson, R. G. (1971). "Glare from Windows". *Construction Research and Development Journal*, Vol. 2, No. 4, pp. 169-175.

Kittler, R. (1986). "Luminance Models of Homogeneous Skies for Design and Energy Performance Prediction". *Proceedings, 2nd. International Daylighting Conference, Atlanta, GA: American Society of Heating, Refrigerating and Air-Conditioning Engineers.*

Mahdavi, A., Pal, V. (1998a) "Empirical Evaluation of Solar Radiation, Sky Luminance, and Daylight Prediction Models". *Proceedings of the 1998 IESNA Annual Conference, New York.*

Mahdavi, A., Pal, V. (1998b). "Toward an Entropy-based Light Distribution Uniformity Indicator". *Proceedings of the 1998 IESNA Annual Conference, New York.*

Mahdavi, A. (1996). "Computational Support for Performance-Based Reasoning in Building Design". *Proceedings of the CIB-ASTM-ISO-RILEM International Symposium "Applications of the Performance Concept in Building"*. Tel Aviv, Israel. Vol. 1, pp. 4.23 - 4.32.

Mahdavi, A., Prankprakma, P., Berberidou, L. (1995). *On Numeric Indicators of Light Distribution Uniformity*. *Proceedings of the 1995 IESNA Annual Conference, New York.* pp. 385 - 394.

Mahdavi, A., Berberidou, L. (1994). "GESTALT: A Prototypical Realization of an Open Daylighting Simulation Environment", *Journal of the Illuminating Engineering Society*, Summer 1994.

Perez, R., R. Seals, and J. Michalsky (1993). "All-Weather Model for Sky Luminance Distribution - Preliminary Configuration and Validation". *Solar Energy* Vol. 50, No. 3, 1993: pp. 235-245.

Perez, R., Ineichen, P., Seals, R., Michalsky, J., and Stewart, R. (1990). "Modeling Daylight Availability and Irradiance Components from Direct and Global Irradiance". *Solar Energy* 44, pp. 271-289.

Sorensen, K. (1991). "Practical Aspects of Discomfort Glare Evaluation: Interior Lighting". *Symposium Proceedings, First International Symposium on Glare, New York*, pp. 55-59.

Tellier, P., Bouatouch, K., (1991) "Physics Based Lighting Models: Implementation Issues", *Photorealistic Rendering in Computer Graphics, 1991*. Berlin: Springer-Verlag.